FRIEDRICH-ALEXANDER-UNIVERSITÄT ERLANGEN-NÜRNBERG
INSTITUT FÜR INFORMATIK (MATHEMATISCHE MASCHINEN UND DATENVERARBEITUNG)

Lehrstuhl für Informatik 10 (Systemsimulation)

Accurate techniques for computing singular solutions of elliptic problems

H. Köstler and U. Rüde

Technical Report 04-3

Abstract

Generalized functions occur in many practical applications as source terms in partial differential equations. Typical examples are point sources and sinks in porous media flow that are described by Dirac δ-functions or point loads and dipoles as source terms for electrostatic potentials.

For analyzing the accuracy of such computations, standard techniques cannot be used, since they rely on global smoothness. This is both true for Sobolev space arguments for finite element based methods, and for continuity and differentiability arguments in finite difference analysis. At the singularity, the solution tends to infinity and therefore standard error norms will not even converge.

In this article we will demonstrate that these difficulties can be overcome by using other metrics to measure accuracy and convergence of the numerical solution. Only minor modifications to the discretization and solver are necessary to obtain the same asymptotic accuracy and efficiency as for regular and smooth solutions. In particular, no adaptive refinement is necessary and it is also unnecessary to use techniques which make use of the analytic knowledge of the singularity. Our method relies simply on a mesh-size dependent representation of the singular sources constructed by appropriate smoothing. It can be proved that the pointwise accuracy is of the same order as in the regular case. The error coefficient depends on the location and will deteriorate when approaching the singularity where the error estimate breaks down. Our approach is therefore useful for accurately computing the global solution, except in a small neighborhood of the singular points. It is also possible to integrate these techniques into a multigrid solver exploiting additional techniques for improving the accuracy, such as Richardson and τ-Extrapolation.

1 Introduction

Typical error estimates for the numerical solution of boundary value problems depend on the smoothness of the true solution which is not given in many practical applications. Reasons for such singular solutions can for example be reentrant corners, discontinuous coefficients, singular functions in the boundary conditions or source terms with singularities. In this article we consider the last case. As application we choose for simplicity electrostatic potentials of point loads, dipoles and quadrupoles, physically modeled by the Maxwell equations in the vacuum (cf. [1]). The method is extensible to more general situations, but the basic idea of the method is presented here in terms of this simple example. It leads to the **Poisson equation** with Dirichlet boundary conditions in the unit cube $\Omega = [0,1]^3 \subset \mathbb{R}^3$

$$\begin{array}{rcll} -\Delta u &=& f & \text{in } \Omega \\ u &=& g & \text{on } \partial\Omega \end{array} , \qquad (1)$$

where Δ is the Laplace operator, $\partial\Omega$ denotes the boundary of Ω and g is a smooth function. The source term f contains one or more singularities, because a point load is modeled by the Dirac δ-function. As an extension we will consider sources containing dipoles and quadrupoles. A dipole can formally introduced as a directional derivative of a point load, a quadrupole as a directional derivative of a dipole. So we have to study the Dirac δ-function and its derivatives in order to solve problem (1). Note that the Dirac δ-function is not a function in the classical sense, but a **distribution** (cf. [2]). The concept of a distribution or generalized function is introduced in section 2.1 (cf. [3]). Throughout the paper we will focus on the case of a single, isolated right-hand-side singularity. The case of several singularities can be studied easily by using the superposition principle. After that we derive in section 2.2 the weak solution of the Poisson equation. For the discretization of (1)

$$\begin{array}{rcll} \Delta_h u_h &=& f_h & \text{in } \Omega_h \\ u_h &=& g_h & \text{on } \partial\Omega_h \end{array} \qquad (2)$$

we use finite differences on equidistant grids

$$\Omega_h = \{(ih, jh, kh), 0 < i < N, 0 < j < N, 0 < k < N \; i,j,k,N \in \mathbb{N}\}$$

with mesh size $h = \frac{1}{N}$. The discrete Laplace operator is given by the usual 7-point stencil

$$\Delta_h \;=\; \delta_x^2 + \delta_y^2 + \delta_z^2 \;, \qquad (3)$$

with the difference operator

$$\delta_x^2 \;=\; \frac{u(x-h,y,z) - 2u(x,y,z) + u(x+h,y,z)}{h^2}$$

and analogous for δ_y^2 and δ_z^2.

The question is now how to discretize the right hand side f containing the singularity. f is equal to zero on every point in Ω except at the singularity where it is ∞. If we assume that the singularity is not located at a grid point, simply set $f_h \equiv 0$ and then try to solve the above problem without any modifications and a standard solver, we would get poor results. On the one hand, standard error norms near the singularity will not converge, because the solution at the singularity is unbounded, and on the other hand the accuracy is destroyed in the whole domain by the singularity. This phenomenon is called **pollution effect**. If the singularity is not located at a grid point we simply set the mesh point next to it to $1/h^2$. This concept leads to a discretization error of order $\mathcal{O}(h)$.

In section 2.3 we present the **Zenger Correction Method**. It improves the order of the discretization error to $\mathcal{O}(h^2)$ except in a small neighborhood of the singularity and overcomes the pollution effect. The idea is to represent the singular generalized components of f by grid-adapted B-Splines. Extending results from [4] we can show that the pollution effect can be eliminated leading to errors of the same quality and convergence rate as for smooth problems. Its great advantage is that we do not need to know the exact singular component of the solution of the problem to approximate the singularity. Therefore it can be used for a variety of problems.

In section 3 the core theorems for the error estimates of the discretization error for the Poisson equation in the unit cube are presented and the proof of the main result is outlined.

In section 4 we further improve the accuracy of the numerical solution by using extrapolation. Two extrapolation methods, namely Richardson extrapolation and τ-extrapolation are briefly described in combination with the Zenger Correction.

In the 5th section the experimental results for the numerical solution of the Poisson equation with Zenger Correction and extrapolation for 3 dimensions are summarized.

2 Singular source terms in Poisson's equation

2.1 Distributions

First we introduce generalized functions that are an extension to the usual mathematical functions (cf. [5, 6]).

Definition 1 (Test function)
A ***test function*** $\phi : \mathbb{R}^n \to \mathbb{R}$ *is a function which is infinitely differentiable on* $\mathbb{R}^n$ *(this means that every partial derivative to every order exists) and vanishes outside some bounded region (which may vary from test function to test function). The space of all test functions on* $\mathbb{R}^n$ *will be denoted by* $C_0^\infty(\mathbb{R}^n)$*.*

Definition 2 (Distributions) *We say that* f *is a* ***linear functional*** *on* $C_0^\infty(\mathbb{R}^n)$ *if there exists a rule which assigns to each* $\phi(\mathbf{x}) \in C_0^\infty(\mathbb{R}^n)$ *a real number denoted by* $\langle f, \phi\rangle$ *such that*

$$\langle f, \alpha_1\phi_1 + \alpha_2\phi_2\rangle = \alpha_1\langle f, \phi_1\rangle + \alpha_2\langle f, \phi_2\rangle$$

$\forall \alpha_1, \alpha_2 \in \mathbb{R}$ *and* $\forall \phi_1, \phi_2 \in C_0^\infty(\mathbb{R}^n)$*. A linear functional is said to be continuous if, whenever* $\{\phi_m\}$ *is a null sequence in* $C_0^\infty(\mathbb{R}^n)$*, the numerical sequence* $\langle f, \phi_m\rangle$ *tends to* 0 *as* $m \to \infty$*. A continuous linear functional on* $C_0^\infty(\mathbb{R}^n)$ *is said to be a* ***distribution*** *or* ***generalized function****. The number* $\langle f, \phi\rangle$ *is the value of* f *at* ϕ*.*

Definition 3 (Locally integrable) *A function* $f : \mathbb{R}^n \to \mathbb{R}$ *is said to be* ***locally integrable*** *if* $\int_\Omega |f| dx$ *exists for every bounded domain* $\Omega \subset \mathbb{R}^n$*.*

Theorem 1 *A locally integrable function* $f : \mathbb{R}^n \to \mathbb{R}$ *generates an n-dimensional distribution* f *through the rule*

$$\langle f, \phi\rangle = \int_{\mathbb{R}^n} f(\mathbf{x})\phi(\mathbf{x})d\mathbf{x} \tag{4}$$

Proof: found in [2].

A distribution is called **regular** if it can be written in the form (4), otherwise it is called **singular**. Next we show how to differentiate distributions.

Theorem 2 *If $f : \mathbb{R}^n \to \mathbb{R}$ is a differentiable function whose first derivative $f'(x)$ is locally integrable, f' defines its own distribution*

$$\langle f', \phi \rangle \;=\; \int_{-\infty}^{\infty} f'(x)\phi(x)dx \;=\; -\int_{-\infty}^{\infty} f(x)\phi'(x)dx \;=\; \langle f, -\phi' \rangle$$

Proof: The theorem follows with (4) and the middle step is a result of integration by parts combined with the fact that $\phi \equiv 0$ outside a bounded interval.

The last theorem can be extended to arbitrary distributions (cf. [2], p.108).

Definition 4 (Differentiation of distributions) *We define the* ***partial derivatives of an n-dimensional distribution*** *f by*

$$\langle \frac{\partial f}{\partial x_i}, \varphi \rangle = \langle f, -\frac{\partial \varphi}{\partial x_i} \rangle \quad . \tag{5}$$

If we use this definition several times we have the ***derivative of an n-dimensional distribution*** *f*

$$\langle D^{\mathbf{k}} f, \varphi \rangle = (-1)^{|\mathbf{k}|} \langle f, -D^{\mathbf{k}} \varphi \rangle \quad , \tag{6}$$

where $\mathbf{k} = (k_1, \ldots, k_n)$ for $k_1, k_2, \ldots k_n \in \mathbb{N}_0$ is called the ***multi index of dimension*** *n. Furthermore $|\mathbf{k}| = k_1 + k_2 + \cdots + k_n$ and*

$$D^{\mathbf{k}} = \frac{\partial^{|\mathbf{k}|}}{\partial x_1^{k_1} \partial x_2^{k_2} \cdots \partial x_n^{k_n}} \quad . \tag{7}$$

From now on we will use derivatives in the **distributional sense**. Further details on distributions are e.g. found in [7] or [2].

2.2 (Weak) solutions of the Poisson equation with distributions on the right hand side

In order to emphasize that we consider distributions rather than functions we use the term **weak solution**. To obtain the weak solutions of the Poisson equation on the n-dimensional unit sphere $\Omega^n \subset \mathbb{R}^n$ with a point load as source term we use **rotationally symmetric harmonic functions** that depend only on $|\mathbf{x}| = r$ and which satisfy the Laplace equation $\Delta u = 0$ for $r \neq 0$ (cf. [3], S.64). They have the form (cf. [3], pp.138)

$$\gamma_n(\mathbf{x}) = \begin{cases} \dfrac{1}{(2-n)\omega_n} r^{2-n} & : \quad n \neq 2 \\ \dfrac{1}{2\pi} \ln r & : \quad n = 2 \end{cases} \quad . \tag{8}$$

Here

$$\omega_n = \frac{2\pi^{n/2}}{\Gamma(n/2)} \tag{9}$$

is the surface of the n-dimensional unit sphere and Γ is the **gamma function**. In the distributional sense γ_n satisfies the equation

$$\Delta \gamma_n = \delta \quad . \tag{10}$$

This is proved in [3]. Therefore γ_n is a weak solution of the Poisson equation with a point load as source term.

2.3 Grid dependent numerical approximations of singular distributions

The **Zenger Correction Method** uses the following generalized functions in order to approximate the physical singularities δ in equation (10).

Definition 5 (Generalized functions H_i) *Let $H_0 : \mathbb{R} \to \mathbb{R}$ be the* ***Heaviside-function***

$$H_0(x) := \begin{cases} 0 & : \quad x \le 0 \\ 1 & : \quad x > 0 \end{cases} , \tag{11}$$

and the distributions H_i, $i \in \mathbb{Z}$, be recursively defined by

$$H_i(x) := \begin{cases} \frac{d}{dx} H_{i-1}(x) & : \quad i > 0 \\ \int_{-\infty}^{x} H_{i+1}(\xi) d\xi & : \quad i < 0 \end{cases} . \tag{12}$$

Figure 1 illustrates three of these distributions.

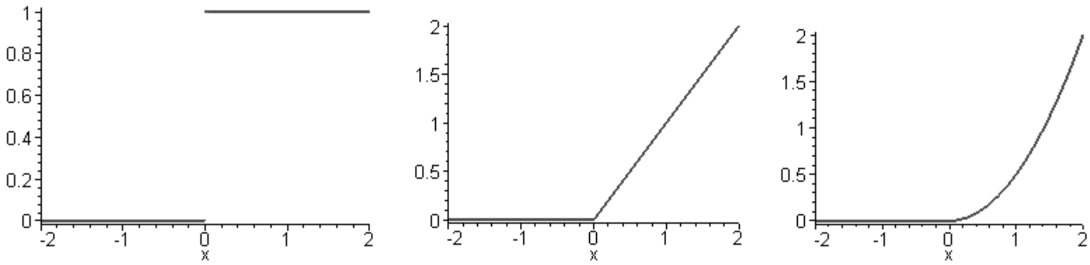

Figure 1: The functions H_0, H_{-1} and H_{-2}.

Remark 1 *For $i \le 0$ we the H_i are classical functions and for $i < 0$ we obtain with*

$$(x-y)_+^0 = \begin{cases} 1 & : \quad x \ge y \\ 0 & : \quad x < y \end{cases} \tag{13}$$

and

$$(x-y)_+^m = \begin{cases} (x-y)^m & : \quad x \ge y,\, m > 0 \\ 0 & : \quad x < y \end{cases} \tag{14}$$

that

$$H_i(x) = \frac{(x)_+^{|i|}}{|i|!} . \tag{15}$$

The family of functions H_i enables us to represent arbitrary physical multipoles. For example H_1 corresponds to the Dirac δ-function resp. a point load. Remember that the directional derivative of a point load was defined as a special dipole. For higher dimensions we use tensor products of these functions. In 3D for example a point load at $\mathbf{x}_0 = (x_0, y_0, z_0)^T$ is therefore described by

$$H_1(x-x_0)H_1(y-y_0)H_1(z-z_0) := \mathcal{H}^{1,1,1}_{x_0,y_0,z_0}(\mathbf{x}) . \tag{16}$$

Generally we use multi indices $\mathbf{x}_0 = (x_{0,1}, x_{0,2}, \ldots, x_{0,n}) \in \mathbb{R}^n$ to indicate the location of the singularity and $\mathbf{a} = (a_1, a_2, \ldots, a_n) \in \mathbb{Z}^n$ to specify the order and use the notation

$$\mathcal{H}^{\mathbf{a}}_{\mathbf{x}_0}(\mathbf{x}) := \prod_{i=1}^{n} H_{a_i}(x_i - x_{0,i}) . \tag{17}$$

Given $\mathbf{v} \in \mathbb{R}^3$, $\|\mathbf{v}\| = 1$, the directional derivative of term (16) leads to a dipole in 3D

$$\mathbf{v} \cdot \nabla \mathcal{H}^{(1,1,1)}_{\mathbf{x}_0}(\mathbf{x}) = \mathbf{v} \cdot \begin{pmatrix} H_2(x-x_0)H_1(y-y_0)H_1(z-z_0) \\ H_1(x-x_0)H_2(y-y_0)H_1(z-z_0) \\ H_1(x-x_0)H_1(y-y_0)H_2(z-z_0) \end{pmatrix} . \tag{18}$$

The idea of the Zenger Correction Method is now to **integrate** the right hand side f **analytically** a number of times, until the result is a product of (classical) functions H_i with $i < 0$. Then we **differentiate** this function **numerically** as often as it had been integrated. This results in a smooth approximation to the distribution f that depends on the meshsize h and becomes more accurate with smaller h.

For the example of a point load in 3D, that is $f = \mathcal{H}_{\mathbf{x}_0}^{(1,1,1)}(\mathbf{x})$, we integrate twice in each direction. This leads to $\mathcal{H}_{\mathbf{x}_0}^{(-1,-1,-1)}(\mathbf{x})$. For the numerical differentiation we use finite differences with the notation

$$\delta^{\mathbf{i}} = \delta_{x_1}^{i_1} \circ \delta_{x_2}^{i_2} \circ \cdots \circ \delta_{x_n}^{i_n} \quad , \tag{19}$$

for the multi index $\mathbf{i} \in \mathbb{Z}^n$ that indicates how often we differentiate in each direction. Now the source term of the discrete Poisson equation has to be replaced by $f_h = \delta^{(2,2,2)}\mathcal{H}_{\mathbf{x}_0}^{(-1,-1,-1)}(\mathbf{x})$. Dependent on the number of integrations resp. differentiation steps n we call this procedure the **Zenger Correction of n-th order**. For the dipole with direction $\mathbf{v}$ in 3D, the Zenger correction of 4th order leads to the approximation

$$f_h = \mathbf{v} \cdot \begin{pmatrix} \delta^{(4,4,4)}\mathcal{H}_{\mathbf{x}_0}^{(-2,-3,-3)}(\mathbf{x}) \\ \delta^{(4,4,4)}\mathcal{H}_{\mathbf{x}_0}^{(-3,-2,-3)}(\mathbf{x}) \\ \delta^{(4,4,4)}\mathcal{H}_{\mathbf{x}_0}^{(-3,-3,-2)}(\mathbf{x}) \end{pmatrix} \quad .$$

Theorem 3 *In general for even n with $k - n < 0$ we obtain*

$$\delta_x^n H_k(x) = \begin{cases} 0 & : \quad |x| \geq \frac{n}{2}h \\ \frac{1}{h^n}\sum_{i=0}^{n}(-1)^i \begin{pmatrix} n \\ i \end{pmatrix} H_{k-n}(x + (i - \frac{n}{2})h) & : \quad |x| < \frac{n}{2}h \end{cases} \quad . \tag{20}$$

In [8] it is shown that formula (20) in fact is the nth numerical derivative of $H_k(x)$ and that it is equal to a B-Spline.

3 Error estimates

In this section we prove that if the singularity in the source term is replaced by the above approximation, we obtain an $O(h^2)$ discretization error as in the smooth case, except in a small neighborhood of the singularity.

3.1 Asymptotic expansion of the error in the smooth case

First we consider the smooth case without singularities and derive an asymptotic expansion for the discretization error. We start with some definitions (cf. [9], p. 8).

Definition 6 (Asymptotic sequence) *A finite or infinite sequence of functions $\{\Phi_n(x)\}$, defined in a pointed neighborhood of x_0 is called an **asymptotic sequence** as $x \to x_0$ if the following two conditions are satisfied*

1. $\Phi_n(x) \neq 0, \quad x \neq x_0 \wedge n \in \mathbb{N}$
2. $\Phi_{n+1}(x) = o(\Phi_n(x)), \quad x \to x_0$

The most common example of an asymptotic sequence for $x_0 \in \mathbb{R}$ is $\{(x - x_0)^n\}$. For meshsize h we have $x = x_0 + h$ and thus $\{h^n\}$.

Definition 7 (Asymptotic expansion) *Let $\{\Phi_n(x)\}$ be an asymptotic sequence as $x \to x_0$. A function $f(x)$ has an **asymptotic development** to N terms with respect to the sequence $\{\Phi_n(x)\}$ if there exist constants $c_1, \ldots, c_N$ such that*

$$f(x) = c_1\Phi_1(x) + \cdots + c_N\Phi_N(x) + o(\Phi_N(x)), \quad x \to x_0 \quad . \tag{21}$$

In the case where $f(x)$ has an expansion to N terms for every N we say that $f(x)$ has an ***asymptotic expansion*** *in terms of the sequence $\{\Phi_n(x)\}$ and write*

$$f(x) \sim \sum_{n=1}^{\infty} c_n \Phi_n(x), \quad x \to x_0 \ . \tag{22}$$

Remark 2 *In relation (21) the error is of smaller order than the last retained term. In the case of an expansion to all orders the expression $o(\Phi_N(x))$ becomes $\mathcal{O}(\Phi_{N+1}(x))$.*

More details about asymptotic expansions are e.g. found in [10].

Theorem 4 *Let u^* defined on $\overline{\Omega}$ be the solution of the boundary value problem (1) with homogeneous right hand side*

$$\begin{array}{rcll} \Delta u &=& 0 & \text{in } \Omega \\ u &=& f & \text{on } \partial\Omega \end{array} , \tag{23}$$

where f is bounded and piecewise continuous on the boundary of $\Omega = [0,1]^d, \quad d \in \{2,3\}$. Let u_h^* be a grid function defined on Ω_h solving the discrete analogue of (23)

$$\begin{array}{rcll} \Delta_h u_h &=& 0 & \text{in } \Omega_h \\ u_h &=& f_h & \text{on } \partial\Omega_h \end{array} , \tag{24}$$

where Δ_h is the 7-point stencil defined in (3). Then:

$$u_h^* = u^* + \sum_{l=1}^{p} c_l h^{2l} + \mathcal{O}(h^{2p+2})$$

where $u^* + \sum_{l=1}^{p} c_l h^{2l} + \mathcal{O}(h^{2p+2})$ is restricted to Ω_h and $c_1, c_2, \ldots, c_p$ are bounded on $\overline{\Omega}$.

Proof: Proof is found in [11] for the 2D case and in appendix A for the 3D case.

3.2 h-boundedness

Next we introduce the notation of **h-boundedness**.

Definition 8 (h-bounded) *A family of functions $u_h(\mathbf{x})$ is called h-**bounded** on the domain $\Omega \subset \mathbb{R}^n$, if there exists a real valued, continuous function $r(\mathbf{x})$ on Ω, which is not necessarily bounded on Ω, so that for every $\mathbf{x} \in \Omega$ there exists a number $h_0 > 0$ with $|u_h(\mathbf{x})| \le r(\mathbf{x})$ for all $h = \frac{1}{N} < h_0, N \in \mathbb{N}$, $\mathbf{x} \in \Omega_h$. If $r(\mathbf{x})$ is bounded on Ω, $u_h(\mathbf{x})$ is called **strictly** h-**bounded** (cf. [12], p.6).*

An h-bounded family of grid functions u_h may be unbounded on Ω for $h \to 0$, but because of the continuity of r be bounded for all $h > 0$ on every compact subset of Ω.

Theorem 5 *Let the solution of*

$$\Delta_h u_h = f_h \quad \text{in } \Omega_h$$

be bounded on $\overline{\Omega}_h$. If $\delta^{2\mathbf{i}} f_h$ is h-bounded on Ω and $\forall i_l, m_l$ with $0 < l \le n$ is $0 \le i_l \le m_l$, then $\delta^{2\mathbf{m}} u_h$ is h-bounded on Ω.

Proof: Proof is found in [13] for the 2D case and in appendix B for the 3D case.

3.3 Main theorem

Now we are prepared for the central theorem. It states that the global pointwise discretization error after the Zenger Correction is $\mathcal{O}(h^2)$ as in the smooth case.

Theorem 6 *Let u^* be the (weak) solution of the boundary value problem*

$$\begin{array}{rcll} \Delta u & = & \mathcal{H}^{\mathbf{a}}_{\mathbf{x}_0}(\mathbf{x}) & \text{in } \Omega \\ u & = & 0 & \text{on } \partial\Omega \end{array} , \tag{25}$$

where $\mathcal{H}^{\mathbf{a}}_{\mathbf{x}_0}(\mathbf{x})$ is a distribution, whose singularity is located at $\mathbf{x}_0 \in \Omega =]0,1[^n$. Let u_h^* the solution of

$$\begin{array}{rcll} \Delta_h u_h & = & f_h & \text{in } \Omega_h \\ u_h & = & 0 & \text{on } \partial\Omega_h \end{array} , \tag{26}$$

where

$$f_h = \delta^{2\mathbf{m}}\, \mathcal{H}^{\mathbf{a}-2\mathbf{m}}_{\mathbf{x}_0}(\mathbf{x}) \ ,$$

and where $\mathbf{m}$ is chosen such that $2m_l > a_l, 1 \le l \le d$. $d \in \{2,3\}$ is the dimension of the problem. Then $\mathcal{H}^{\mathbf{a}-2\mathbf{m}}_{\mathbf{x}}$ are continuous functions and

$$u_h^* = u^* + h^2 r$$

where r is h-bounded on $\Omega\backslash\{\mathbf{x}_0\}$.

The proof can for the 2D case can be found in [4], pp.15. We extend it here to 3D.

Proof: We know from Theorem 4 that smooth boundary values cause (in our simple domain) errors with h^2 expansions. We consider the boundary value problem (25) with boundary conditions

$$u(\mathbf{x}) = u_S^*(\mathbf{x}) \text{ on } \partial\Omega_h \ ,$$

where u_S^* is the analytical solution of the singular problem. The solution is given by

$$u^*(\mathbf{x}) = u_S^*(\mathbf{x}) \ .$$

Now we construct an auxiliary problem by “integrating” the original problem

$$\begin{array}{rcll} \Delta U & = & \mathcal{H}^{\mathbf{a}-2\mathbf{m}}_{\mathbf{x}_0}(\mathbf{x}) & \text{in } \Omega_h \\ U & = & F(\mathbf{x}) & \text{on } \partial\Omega_h \end{array} , \tag{27}$$

where $D^{2\mathbf{m}}F(\mathbf{x}) = u_S^*(\mathbf{x})$ with

$$D^{\mathbf{m}} = \frac{\partial^{|\mathbf{m}|}}{\partial x_1^{m_1}\partial x_2^{m_2}\cdots\partial x_d^{m_d}} \tag{28}$$

and $|\mathbf{m}| = m_1 + m_2 + \cdots + m_n$. (27) is numerically approximated by

$$\begin{array}{rcll} \Delta_h U_h & = & \mathcal{H}^{\mathbf{a}-2\mathbf{m}}_{\mathbf{x}_0}(\mathbf{x}) & \text{in } \Omega_h \\ U_h & = & F(\mathbf{x}) & \text{on } \partial\Omega_h \end{array} . \tag{29}$$

Now we define R as the discretization error for the auxiliary problem (27) and (29), respectively.

$$U_h^* = U^* + h^2 R \ ,$$

where U^* is the analytical solution of (27) and U_h^* is the numerical solution of (29). Note that

$$D^{2\mathbf{m}}U^*(\mathbf{x}) = u^*(\mathbf{x})$$

on $\Omega \setminus \{\mathbf{x}_0\}$. The remainder R satisfies

$$\Delta_h R = Q := \frac{1}{h^2}(\mathcal{H}^{\mathbf{a}-2\mathbf{m}}_{\mathbf{x}_0}(\mathbf{x}) - \Delta_h U^*) \ .$$

Using Taylor-expansions and smoothness properties of U^* for estimating the remainder term we can show that

1. Q is bounded on Ω_h, since there exists a number $R_T \in \mathbb{R}$ with

$$|Q(\mathbf{x})| = |\frac{1}{h^2}(\Delta U^* - \Delta_h U^*)| \leq R_T \ .$$

2. $\delta^{2\mathbf{i}}Q$ is h-bounded on $\Omega\backslash\{\mathbf{x}_0\}$ for all i_l, $0 < l \leq n$.

Because of these two properties, R is bounded on Ω and using Theorem 5 even $\delta^{2\mathbf{n}}R$ is h-bounded on Ω. Now we define $\widetilde{u}_h$ as a auxiliary grid function that is obtained by finite differences applied to U_h

$$\widetilde{u}_h := \delta^{2\mathbf{m}}U_h \text{ in } \Omega_h \ ,$$

where the necessary values U_h outside Ω_h are chosen such that $\Delta_h \widetilde{U}_h = F(\mathbf{x})$ on the boundary of Ω_h (and sufficiently many points outside Ω_h), too. By construction $\widetilde{u}_h$ satisfies

$$\begin{array}{rcll} \Delta_h \widetilde{u}_h &=& f_h & \text{in } \Omega_h \\ \widetilde{u}_h &=& u_S^*(\mathbf{x}) + h^2\widetilde{r} & \text{on } \partial\Omega_h \end{array} \ , \tag{30}$$

where because of the smoothness of u along the boundary $\widetilde{r}$ is h-bounded. Thus u_h and $\widetilde{u}_h$ are solutions to almost the same numerical boundary value problem. Since 30 differs from (26) only by an $\mathcal{O}(h^2)$ perturbation in the boundary values, we can use the discrete maximum principle and show that u_h and $\widetilde{u}_h$ cannot differ by more than $\mathcal{O}(h^2)$. Furthermore

$$\widetilde{u}_h = \delta^{2\mathbf{m}}U^* + h^2\delta^{2\mathbf{m}}R = u^* + (\delta^{2\mathbf{m}}U^* - u^*) + h^2\delta^{2\mathbf{m}}R \ .$$

Now $\delta^{2\mathbf{n}}U^* - u^*$ and $\delta^{2\mathbf{n}}R$ are h-bounded in $\Omega\backslash\{\mathbf{x}_0\}$. This completes the proof of the theorem.
□

3.4 Summary of Zenger Correction

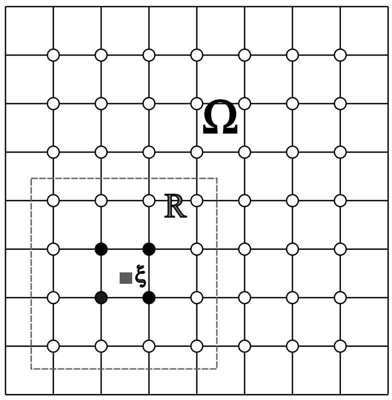

Figure 2: Zenger Correction

Summarizing the Zenger Correction method is recapitulatorily illustrated in figure 2. The right hand side of the Poisson equation (1) is changed in a fixed neighborhood of the location $\mathbf{x}_0$ of the singularity. For example in the case of a point load with Zenger Correction of 2nd order only points with a distance less or equal the mesh size h are corrected by the B-Spline approximation. Since the pollution effect vanishes but the exact solution is still unbounded at the singularity, we must cut out a region $R \subset \Omega$ of fixed size, which contains the singularity when measuring the error. Then Theorem 6 states that in $\Omega\backslash R$ the norm of the discretization error depends on the mesh size with $\mathcal{O}(h^2)$.

The advantages of the Zenger Correction Method are that no modification of the grid or the solver is necessary. Furthermore the number of points that have to be corrected is fixed and does not depend on the mesh size h. No analytical solution is needed to construct the correction.

Note that the Zenger Correction Method eliminates the pollution effect. This results in a (pointwise) $\mathcal{O}(h^2)$ accuracy at any fixed distance from the singular point. However, the method cannot provide good accuracy at the singularity itself and therefore in standard global error norms on Ω. This is impossible since the true solution tends to infinity where the singularity is located. Note that in a standard global norm (like L^∞) the method may not even converge, or may converge only slowly. In the literature (see e.g. [14]) special weighted norms are constructed to deal with singularities. The construction of such norms is dependent on the singularity. In contrast, our approach works for any singularity that is represented by a distribution and R can be chosen arbitrarily small. This will not affect the order of convergence, but only the constants in the estimate.

4 Extrapolation

Up to now we have a discretization error of order $\mathcal{O}(h^2)$. In this section we present two extrapolation methods in order to improve the discretization error to $\mathcal{O}(h^4)$.

4.1 Richardson Extrapolation

Richardson Extrapolation can be used if there exist asymptotic expansions of the discretization error (cf. [15]). In this case the solutions of different mesh sizes can be combined to eliminate the lower order terms. For our problem we use the mesh sizes h and $H = 2h$. In order to get the higher accuracy on the coarse grid we change the values there by

$$\widehat{\mathbf{u}}_H^* = \frac{4}{3}\mathcal{I}_h^H \mathbf{u}_h^* - \frac{1}{3}\mathbf{u}_H^* \ , \tag{31}$$

where $\mathcal{I}_h^H$ is an injection operator. The existence of such asymptotic expansions was proved in Theorem 6.

4.2 τ-Extrapolation

τ-Extrapolation is a multigrid specific technique that in contrast to Richardson extrapolation works only on a single grid. It is based on the principle of **defect correction** and has been first mentioned by Brandt (cf. [16], see also Hackbusch [17], pp.278).

In the CS(correction scheme)-Multigrid algorithm two different iterations are used alternately, the smoother and the coarse grid correction (cf. [18]). These two iterations have a common fixed point described by $\mathbf{f}_h - \mathbf{A}_h\mathbf{u}_h = 0$ (cf. [4], p. 17f). The smoother converges fast for certain (usually the high frequency) solution components, but converges only slowly for the remaining (low frequency) modes. The coarse grid correction behaves vice versa. If these complementary properties are combined the typical multigrid efficiency is obtained.

Now we follow the idea of **double discretization**, i.e. in the coarse grid correction process higher order discretizations are used. Using a correction of the form

$$\mathbf{u}_h^{(k+1)} = \mathbf{u}_h^{(k)} + \mathbf{e}_h^{(k)} \ , \tag{32}$$

where $\mathbf{e}_h^{(k)}$ is computed as a coarse grid correction

$$\mathbf{e}_h^{(k)} = \mathcal{I}_H^h \mathbf{A}_H^{-1} \widehat{\mathcal{I}}_h^H (\mathbf{f}_h - \mathbf{A}_h \mathbf{u}_h^{(k)}) \ , \tag{33}$$

would lead to a standard multigrid method. τ-extrapolation consists in using a linear combination of fine and coarse grid residual to construct an extrapolated correction

$$\widehat{\mathbf{u}}_h^{(k+1)} = \mathbf{u}_h^{(k)} + \mathcal{I}_H^h \mathbf{A}_H^{-1} (\frac{4}{3}\widehat{\mathcal{I}}_h^H (\mathbf{f}_h - \mathbf{A}_h \mathbf{u}_h^{(k)}) - \frac{1}{3}(\widehat{\mathcal{I}}_h^H \mathbf{f}_h - \mathbf{A}_H \mathcal{I}_h^H \mathbf{u}_h^{(k)})) \ . \tag{34}$$

It can be shown that this modification of the coarse grid correction leads to a numerical error of order $\mathcal{O}(h^4)$ (cf. [19]). The modified coarse grid correction is only applied on the finest grid once per V-cycle. Additionally we have to take care when choosing the restriction and the interpolation operators. Normally trilinear interpolation for $\mathcal{I}_H^h$, full weighting for $\widehat{\mathcal{I}}_h^H$ and injection for $\mathcal{I}_h^H$ is used, but this can vary from problem to problem. One has also to pay attention not do do too many post smoothing steps, because this can destroy the higher accuracy. For the Poisson equation with singular source term we have to discretize the right hand side on each grid due to the fact that the restriction of the B-spline cannot approximate the right hand side well enough on the coarse grid. A concise analysis of the τ-extrapolation is e.g. found in [19].

5 Experimental results in 3D

For the experiments we use CS-Multigrid as solver, e.g $CS(2,2,15)$ means that we do 2 presmoothing and 2 post-smoothing steps and a maximum of 15 V-cycles. The singularity is located at $\mathbf{x}_0 = (x_0, y_0, z_0)^T$ in the domain $\Omega = [0,1]^3$. To evaluate the accuracy away from the singularity we will consider $\Omega \setminus R$, where $R = [0.125, 0.375]^3$ is a fixed neighborhood of $\mathbf{x}_0$. At the boundary we add the smooth function

$$g(x,y,z) = \sin(x\pi)\sin(y\pi)\sinh(\sqrt{2}z\pi) \ . \tag{35}$$

5.1 Point load

The solution of the Poisson equation in 3D with a point load as source term is given by

$$u_p^*(\mathbf{x}) = -\frac{1}{4\pi|\mathbf{x}|} \ . \tag{36}$$

Experiment 1 *The boundary value problem with the Zenger Correction of 4th order is described by*

$$\begin{array}{rcll} -\Delta u(\mathbf{x}) & = & \mathcal{H}_{\mathbf{x}_0}^{(1,1,1)}(\mathbf{x}) & \text{in } \Omega \\ u(\mathbf{x}) & = & u_p^*(\mathbf{x}) + g(\mathbf{x}) & \text{on } \partial\Omega \end{array} \tag{37}$$

with its discretization

$$\begin{array}{rcll} -\Delta_h u_h(\mathbf{x}) & = & \delta^{(4,4,4)}\mathcal{H}_{\mathbf{x}_0}^{(-3,-3,-3)}(\mathbf{x}) & \text{in } \Omega_h \\ u_h(\mathbf{x}) & = & u_{p,h}^*(\mathbf{x}) + g_h(\mathbf{x}) & \text{on } \partial\Omega_h \end{array} \ . \tag{38}$$

Table 1 lists the numerical results. The first column shows the mesh size h, the second the maximum norm of the discretization error, then follow the L_1 resp. L_2 norms in the whole domain Ω and in the domain $\Omega\backslash R$. The small numbers between the rows of the table show the numerical convergence rates α which are for a point $\mathbf{p} \in \Omega$ computed by

$$\alpha = (\ln|u^*(\mathbf{p}) - u_h(\mathbf{p})| - \ln|u^*(\mathbf{p}) - u_{h/2}(\mathbf{p})|)/(\ln 2) \tag{39}$$

and analogous for the norms in the other columns.

Table 1: Convergence rates of the discretization error for the Poisson equation in 3D with a point load at $\mathbf{x}_0 = (0.26, 0.26, 0.26)^T$, Zenger Correction of 4th order, $g = \sin(x\pi)\sin(y\pi)\sinh(\sqrt{2}z\pi)$, solver $CS(2,2,15)$.

h	$(\frac{1}{2},\frac{1}{2},\frac{1}{2})$		L_∞	L_1 Ω		L_2 Ω		L_1 $\Omega\backslash R$		L_2 $\Omega\backslash R$	
$\frac{1}{16}$	4.81e-02		2.67e+00	2.04e-02		5.28e-02		1.98e-02		2.61e-02	
		2.0			2.1		2.4		2.1		2.1
$\frac{1}{32}$	1.21e-02		1.22e+00	4.61e-03		9.89e-03		4.52e-03		6.22e-03	
		2.0			2.0		1.2		2.1		2.0
$\frac{1}{64}$	3.02e-03		1.69e+00	1.12e-03		4.34e-03		1.08e-03		1.52e-03	
		2.0			2.0		-0.2		2.0		2.0
$\frac{1}{128}$	7.55e-04		6.92e+00	2.78e-04		5.07e-03		2.63e-04		3.74e-04	
		2.0			2.0		1.9		2.0		2.0
$\frac{1}{256}$	1.89e-04		3.21e+00	6.91e-05		1.39e-03		6.50e-05		9.30e-05	

Experiment 2 *Using an additional Richardson Extrapolation for solving problem (37) we get table 2. τ-extrapolation gives Table 3. discussion of results. Figure 3 visualizes the convergence rates of the Zenger Correction with and without extrapolation in the domain $\Omega\backslash R$ in the L_1-Norm.*

Table 2: Convergence rates of the discretization error for the Poisson equation in 3D with a point load at $\mathbf{x}_0 = (0.26, 0.26, 0.26)^T$, Zenger Correction of 4th order, $g = \sin(x\pi)\sin(y\pi)\sinh(\sqrt{2}z\pi)$, Richardson extrapolation, solver $CS(2, 2, 15)$.

h	$(\frac{1}{2}, \frac{1}{2}, \frac{1}{2})$	L_∞	L_1 Ω	L_2 Ω	L_1 $\Omega\backslash R$	L_2 $\Omega\backslash R$
$\frac{1}{16}$	5.77e-05	7.30e-01	3.89e-04	1.28e-02	3.44e-05	5.32e-05
	4.0		3.6	2.9	3.9	3.5
$\frac{1}{32}$	3.70e-06	2.55e-01	3.19e-05	1.69e-03	2.28e-06	4.66e-06
	4.0		2.4	1.0	3.9	3.7
$\frac{1}{64}$	2.33e-07	3.79e-01	6.14e-06	8.71e-04	1.48e-07	3.56e-07
	4.0		1.6	-0.0	4.0	3.9
$\frac{1}{128}$	1.44e-08	1.03e+00	1.97e-06	8.77e-04	9.21e-09	2.36e-08

Table 3: Convergence rates of the discretization error for the Poisson equation in 3D with a point load at $\mathbf{x}_0 = (0.26, 0.26, 0.26)^T$, Zenger Correction of 4th order, $g = \sin(x\pi)\sin(y\pi)\sinh(\sqrt{2}z\pi)$, τ-extrapolation, solver $CS(2, 1, 14)$.

h	$(\frac{1}{2}, \frac{1}{2}, \frac{1}{2})$	L_∞	L_1 Ω	L_2 Ω	L_1 $\Omega\backslash R$	L_2 $\Omega\backslash R$
$\frac{1}{16}$	1.67e-03	2.64e+00	2.54e-03	4.57e-02	1.54e-03	2.61e-03
	3.9		3.4	2.6	3.9	3.8
$\frac{1}{32}$	1.12e-04	1.18e+00	2.46e-04	7.43e-03	1.01e-04	1.85e-04
	4.0		2.5	0.9	4.0	3.9
$\frac{1}{64}$	7.24e-06	1.66e+00	4.30e-05	3.94e-03	6.46e-06	1.23e-05
	4.0		2.0	-0.3	4.0	3.9
$\frac{1}{128}$	4.58e-07	6.85e+00	1.10e-05	4.97e-03	4.09e-07	8.00e-07
	4.0		2.3	1.9	4.0	4.0
$\frac{1}{256}$	2.86e-08	3.09e+00	2.17e-06	1.30e-03	2.55e-08	5.02e-08

5.2 Dipole

The analytical solution for the Poisson equation is in that case

$$u_d^*(\mathbf{x}) = \frac{\mathbf{v} \cdot \mathbf{x}}{4\pi|\mathbf{x}|^3} \quad , \tag{40}$$

where we choose $\mathbf{v} = (0.5, 0.5, \sqrt{1/2})^T \approx (0.5, 0.5, 0.71)^T$ with $\|\mathbf{v}\|_2 = 1$.

Experiment 3 *We look at the boundary value problem*

$$\begin{aligned} -\Delta u(\mathbf{x}) &= \mathbf{v} \cdot \begin{pmatrix} \mathcal{H}_{\mathbf{x}_0}^{(2,1,1)}(\mathbf{x}) \\ \mathcal{H}_{\mathbf{x}_0}^{(1,2,1)}(\mathbf{x}) \\ \mathcal{H}_{\mathbf{x}_0}^{(1,1,2)}(\mathbf{x}) \end{pmatrix} && \text{in } \Omega \\ u(\mathbf{x}) &= u_d^*(\mathbf{x}) + g(\mathbf{x}) && \text{on } \partial\Omega \end{aligned} \tag{41}$$

with the discretization (using Zenger Correction of 4th order)

$$\begin{aligned} -\Delta_h u_h(\mathbf{x}) &= \mathbf{v} \cdot \begin{pmatrix} \delta^{(4,4,4)}\mathcal{H}_{\mathbf{x}_0}^{(-2,-3,-3)}(\mathbf{x}) \\ \delta^{(4,4,4)}\mathcal{H}_{\mathbf{x}_0}^{(-3,-2,-3)}(\mathbf{x}) \\ \delta^{(4,4,4)}\mathcal{H}_{\mathbf{x}_0}^{(-3,-3,-2)}(\mathbf{x}) \end{pmatrix} && \text{in } \Omega_h \\ u_h(\mathbf{x}) &= u_{d,h}^*(\mathbf{x}) + g_h(\mathbf{x}) && \text{on } \partial\Omega_h \end{aligned} \quad . \tag{42}$$

Table 4 shows the errors. An interesting fact is the high convergence rate of 3 *in the L_1-Norm in the domain Ω. It results from the closeness of the singularity to the next mesh point. The exact solution reaches a very high value there, that causes a high numerical error. The maximum norm of the discretization error therefore stays approximately the same at the point next to the singularity and is higher than the sum of the errors of all the other points so the L_1-norm is determined by this one value. In the domain $\Omega\backslash R$ we have the expected convergence rate $\alpha = 2$.*

Experiment 4 *Additional Richardson extrapolation in (41) results in table 5. If τ-extrapolation is used, we get table 6. Figure 4 again compares the Zenger Correction with and without extrapolation.*

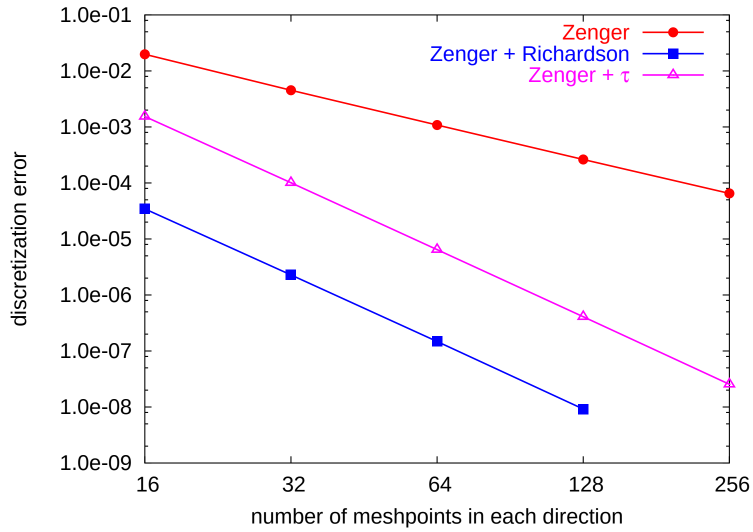

Figure 3: Discretization errors of the Zenger Correction with and without Richardson resp. τ-extrapolation for a point load in 3D in the L_1-Norm in the domain $\Omega \backslash R$

Table 4: Convergence rates of the discretization error for the Poisson equation in 3D with a dipole at $\mathbf{x}_0 = (0.2501, 0.2501, 0.2501)^T$ in direction $\mathbf{v} = (0.5, 0.5, 0.71)^T$, Zenger Correction of 4th order, $g = \sin(x\pi)\sin(y\pi)\sinh(\sqrt{2}z\pi)$, solver $CS(2, 2, 12)$.

h	$(\frac{1}{2}, \frac{1}{2}, \frac{1}{2})$	rate	L_∞	L_1 Ω	rate	L_2 Ω	rate	L_1 $\Omega\backslash R$	rate	L_2 $\Omega\backslash R$	rate
$\frac{1}{16}$	4.30e-02		2.62e+06	7.76e+02		4.51e+04		2.11e-02		2.80e-02	
		2.0			3.1		1.6		2.1		1.9
$\frac{1}{32}$	1.07e-02		2.62e+06	8.79e+01		1.52e+04		5.05e-03		7.38e-03	
		2.0			3.1		1.5		2.0		1.9
$\frac{1}{64}$	2.68e-03		2.62e+06	1.05e+01		5.24e+03		1.24e-03		1.93e-03	
		2.0			3.0		1.5		2.0		2.0
$\frac{1}{128}$	6.70e-04		2.62e+06	1.28e+00		1.83e+03		3.06e-04		4.95e-04	
		2.0			3.0		1.5		2.0		2.0
$\frac{1}{256}$	1.68e-04		2.62e+06	1.59e-01		6.43e+02		7.60e-05		1.25e-04	

5.3 Quadrupole

The analytical solution for a quadrupole as source term is

$$u_q^*(\mathbf{x}) = \frac{\mathbf{w} \cdot \left(|\mathbf{x}|^2 \mathbf{v} - 3\mathbf{x}(\mathbf{v} \cdot \mathbf{x})\right)}{4\pi |\mathbf{x}|^5} \quad . \tag{43}$$

As orthogonal direction of $\mathbf{v} = (0.5, 0.5, \sqrt{1/2})^T$ we compute $\mathbf{w} = (\frac{1}{2}\sqrt{3}, -\frac{1}{6}\sqrt{3}, -\frac{1}{6}\sqrt{6})^T$ with $\|\mathbf{w}\| = 1$.

Experiment 5 *The discretized Poisson equation in 3D with a quadrupole as source term and the Zenger Correction of 4th order is*

$$\begin{array}{rcll} -\Delta_h u_h(\mathbf{x}) &=& \mathbf{w} \cdot (\mathbf{v} \cdot H) & \text{in } \Omega_h \\ u_h(\mathbf{x}) &=& u_{q,h}^*(\mathbf{x}) + g_h(\mathbf{x}) & \text{on } \partial\Omega_h \end{array} \quad , \tag{44}$$

where

$$H = \begin{pmatrix} \delta^{(4,4,4)} \left(\mathcal{H}_{\mathbf{x}_0}^{(-1,-3,-3)}(\mathbf{x}) + \mathcal{H}_{\mathbf{x}_0}^{(-2,-2,-3)}(\mathbf{x}) + \mathcal{H}_{\mathbf{x}_0}^{(-2,-3,-2)}(\mathbf{x})\right) \\ \delta^{(4,4,4)} \left(\mathcal{H}_{\mathbf{x}_0}^{(-2,-2,-3)}(\mathbf{x}) + \mathcal{H}_{\mathbf{x}_0}^{(-3,-1,-3)}(\mathbf{x}) + \mathcal{H}_{\mathbf{x}_0}^{(-3,-2,-2)}(\mathbf{x})\right) \\ \delta^{(4,4,4)} \left(\mathcal{H}_{\mathbf{x}_0}^{(-2,-3,-2)}(\mathbf{x}) + \mathcal{H}_{\mathbf{x}_0}^{(-3,-2,-2)}(\mathbf{x}) + \mathcal{H}_{\mathbf{x}_0}^{(-3,-3,-1)}(\mathbf{x})\right) \end{pmatrix} .$$

Table 5: Convergence rates of the discretization error for the Poisson equation in 3D with a dipole at $\mathbf{x}_0 = (0.2501, 0.2501, 0.2501)^T$ in direction $\mathbf{v} = (0.5, 0.5, 0.71)^T$, Zenger Correction of 6th order, $g = \sin(x\pi)\sin(y\pi)\sinh(\sqrt{2}z\pi)$, Richardson extrapolation, solver $CS(2,2,14)$.

h	$(\frac{1}{2},\frac{1}{2},\frac{1}{2})$		L_∞	L_1 Ω		L_2 Ω		L_1 $\Omega\backslash R$		L_2 $\Omega\backslash R$	
$\frac{1}{16}$	7.81e-05		2.62e+06	7.76e+02		4.51e+04		2.46e-04		1.15e-03	
		3.9			3.1		1.6		3.4		3.2
$\frac{1}{32}$	5.06e-06		2.62e+06	8.79e+01		1.52e+04		2.35e-05		1.22e-04	
		4.0			3.1		1.5		3.7		3.5
$\frac{1}{64}$	3.17e-07		2.62e+06	1.05e+01		5.24e+03		1.79e-06		1.04e-05	
		4.0			3.0		1.5		3.9		3.8
$\frac{1}{128}$	1.98e-08		2.62e+06	1.28e+00		1.83e+03		1.23e-07		7.55e-07	

Table 6: Convergence rates of the discretization error for the Poisson equation in 3D with a dipole at $\mathbf{x}_0 = (0.2501, 0.2501, 0.2501)^T$ in direction $\mathbf{v} = (0.5, 0.5, 0.71)^T$, Zenger Correction of 6th order, $g = \sin(x\pi)\sin(y\pi)\sinh(\sqrt{2}z\pi)$, τ-extrapolation, solver $CS(3,0,13)$.

h	$(\frac{1}{2},\frac{1}{2},\frac{1}{2})$		L_∞	L_1 Ω		L_2 Ω		L_1 $\Omega\backslash R$		L_2 $\Omega\backslash R$	
$\frac{1}{16}$	1.14e-03		2.62e+06	7.76e+02		4.51e+04		3.51e-03		1.61e-02	
		4.1			3.1		1.6		3.3		3.0
$\frac{1}{32}$	6.55e-05		2.62e+06	8.79e+01		1.52e+04		3.69e-04		2.08e-03	
		4.0			3.1		1.5		3.5		3.2
$\frac{1}{64}$	4.05e-06		2.62e+06	1.05e+01		5.24e+03		3.20e-05		2.25e-04	
		3.4			3.0		1.5		3.8		3.6
$\frac{1}{128}$	3.88e-07		2.62e+06	1.28e+00		1.83e+03		2.38e-06		1.82e-05	
		2.4			3.0		1.5		3.7		3.8
$\frac{1}{256}$	7.38e-08		2.62e+06	1.59e-01		6.43e+02		1.86e-07		1.29e-06	

The results are presented in table 7. Richardson Extrapolation leads to table 8 and τ-Extrapolation to table 9. Because of the strong singularity and the high order of the Zenger Correction the convergence rates, as illustrated in graph 5, turn out to be lower for small mesh sizes.

Table 7: Convergence rates of the discretization error for the Poisson equation in 3D with a quadrupole at $\mathbf{x}_0 = (0.26, 0.26, 0.26)^T$ in directions $\mathbf{v} = (0.5, 0.5, 0.71)^T$ and $\mathbf{w} = (0.87, -0.29, -0.41)^T$, Zenger Correction of 4th order, $g = \sin(x\pi)\sin(y\pi)\sinh(\sqrt{2}z\pi)$, solver $CS(2,2,14)$.

h	$(\frac{1}{2},\frac{1}{2},\frac{1}{2})$		L_∞	L_1 Ω		L_2 Ω		L_1 $\Omega\backslash R$		L_2 $\Omega\backslash R$	
$\frac{1}{16}$	5.65e-02		4.46e+03	1.75e+00		7.71e+01		6.06e-02		2.02e-01	
		2.0			1.9		1.4		1.7		1.3
$\frac{1}{32}$	1.44e-02		4.26e+03	4.86e-01		3.01e+01		1.84e-02		8.46e-02	
		2.0			0.1		-1.3		1.8		1.6
$\frac{1}{64}$	3.64e-03		2.32e+04	4.66e-01		7.36e+01		5.13e-03		2.70e-02	
		2.0			-0.1		-2.1		1.9		1.8
$\frac{1}{128}$	9.09e-04		4.16e+05	5.06e-01		3.16e+02		1.36e-03		7.63e-03	
		2.0			0.1		-1.0		2.0		1.9
$\frac{1}{256}$	2.28e-04		1.63e+06	4.83e-01		6.50e+02		3.46e-04		2.02e-03	

6 Conclusion

We have presented here the basic idea of the Zenger Correction Method including some simple examples. More examples, i.e. problems with dipoles and quadrupoles can be found in [8].

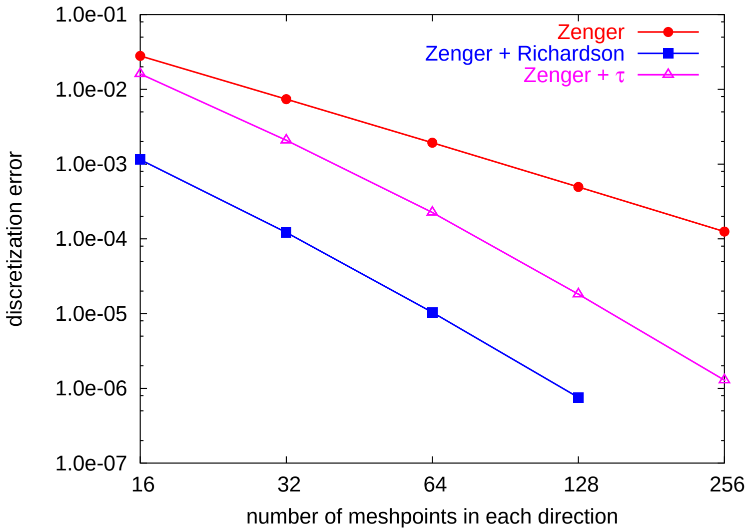

Figure 4: Discretization errors of the Zenger Correction with and without Richardson resp. τ-extrapolation for a dipole in 3D in the L_2-Norm in the domain $\Omega\backslash R$

Table 8: Convergence rates of the discretization error for the Poisson equation in 3D with a quadrupole at $\mathbf{x}_0 = (0.26, 0.26, 0.26)^T$ in directions $\mathbf{v} = (0.5, 0.5, 0.71)^T$ and $\mathbf{w} = (0.87, -0.29, -0.41)^T$, Zenger Correction of 6th order, $g = \sin(x\pi)\sin(y\pi)\sinh(\sqrt{2}z\pi)$, Richardson extrapolation, solver $CS(2, 2, 12)$.

h	$(\frac{1}{2}, \frac{1}{2}, \frac{1}{2})$		L_∞	L_1 Ω		L_2 Ω		L_1 $\Omega\backslash R$		L_2 $\Omega\backslash R$	
$\frac{1}{16}$	5.24e-04		4.42e+03	1.49e+00		7.61e+01		6.32e-03		3.98e-02	
		3.9			2.7		1.9		3.3		3.0
$\frac{1}{32}$	3.49e-05		3.54e+03	2.34e-01		2.10e+01		6.64e-04		5.09e-03	
		4.0			0.4		-0.8		3.6		3.5
$\frac{1}{64}$	2.21e-06		1.72e+04	1.81e-01		3.73e+01		5.55e-05		4.59e-04	
		4.0			-0.7		-2.8		3.8		3.7
$\frac{1}{128}$	1.38e-07		3.74e+05	2.95e-01		2.64e+02		3.96e-06		3.47e-05	

Table 9: Convergence rates of the discretization error for the Poisson equation in 3D with a quadrupole at $\mathbf{x}_0 = (0.26, 0.26, 0.26)^T$ in directions $\mathbf{v} = (0.5, 0.5, 0.71)^T$ and $\mathbf{w} = (0.87, -0.29, -0.41)^T$, Zenger Correction of 8th order, $g = \sin(x\pi)\sin(y\pi)\sinh(\sqrt{2}z\pi)$, τ-extrapolation, solver $CS(5, 0, 15)$.

h	$(\frac{1}{2}, \frac{1}{2}, \frac{1}{2})$		L_∞	L_1 Ω		L_2 Ω		L_1 $\Omega\backslash R$		L_2 $\Omega\backslash R$	
$\frac{1}{16}$	5.66e-03		4.47e+03	2.01e+00		7.77e+01		4.83e-02		2.16e-01	
		4.5			1.5		1.1		2.2		1.2
$\frac{1}{32}$	2.51e-04		4.43e+03	7.00e-01		3.68e+01		1.07e-02		9.54e-02	
		3.9			0.1		-1.4		3.5		3.6
$\frac{1}{64}$	1.63e-05		2.91e+04	6.66e-01		9.57e+01		9.35e-04		8.12e-03	
		3.9			-0.1		-1.9		3.8		3.9
$\frac{1}{128}$	1.11e-06		4.25e+05	6.98e-01		3.56e+02		6.58e-05		5.48e-04	
		4.1			0.0		-1.2		2.3		3.4
$\frac{1}{256}$	6.37e-08		2.16e+06	6.79e-01		8.41e+02		1.29e-05		5.20e-05	

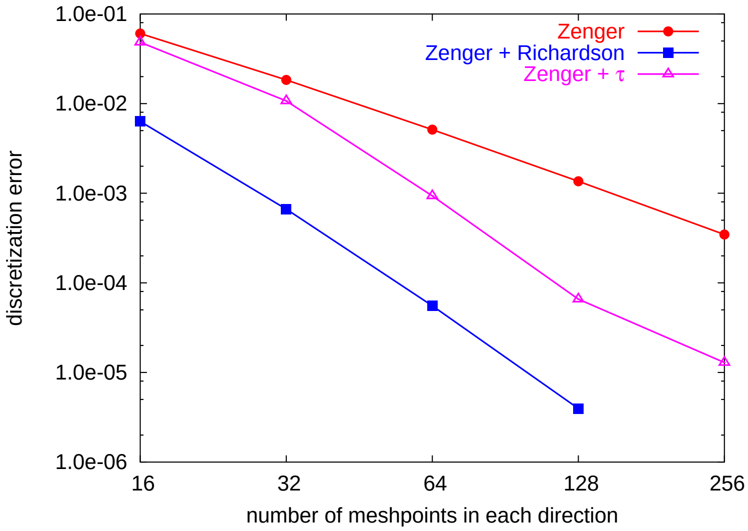

Figure 5: Discretization errors of the Zenger Correction with and without Richardson resp. τ-extrapolation for a quadrupole in 3D in the L_1-Norm in the domain $\Omega \backslash R$

A Proof of Theorem 4

We will now show that for problem (23) smooth boundary values cause errors with h^2 expansions. For the 2D case this was shown in [11]. Our goal is to derive an asymptotic expansion of the discretization error in order to prove Theorem 4.

Because of the linearity of (23) and (24) we can use the superposition principle. Without loss of generality it is sufficient to consider instead of $f(x, y, z)$ only boundary conditions $f_1(x, y, 0)$ that vanish at all but one of the faces of Ω. The general case can easily be obtained by the superposition principle. In the following we set $f(x, y) = f_1(x, y, 0)$ and assume that f is bounded on $\overline{\Omega}$ with $|f(x, y)| \leq M$. Thus we have

$$\begin{array}{rcll} \Delta u(x,y,z) &=& 0 & \text{in } \Omega \\ u(x,y,z) &=& 0 & \text{on } \partial\Omega \ , \quad z>0 \\ u(x,y,0) &=& f(x,y) & \text{on } \partial\Omega \ , \quad z=0 \end{array} \quad . \tag{45}$$

The analytical solution u^* of (45) can then be constructed by a separation ansatz and Fourier series expansion as

$$\begin{array}{rcll} u^*(x,y,z) &=& \displaystyle\sum_{m=1}^{\infty}\sum_{n=1}^{\infty} a_{mn}\sin(m\pi x)\sin(n\pi y)T(t_{mn},z) & \text{for} \quad 0\leq x,y\leq 1, \quad z>0 \\ u^*(x,y,z) &=& f(x,y) & \text{for} \quad 0\leq x,y\leq 1, \quad z=0 \end{array} \ , \tag{46}$$

where $t_{mn} = \sqrt{m^2 + n^2}$,

$$T(t_{mn},z) = \frac{\sinh(\sqrt{m^2+n^2}\pi(1-z))}{\sinh(\sqrt{m^2+n^2}\pi)} \tag{47}$$

$$= e^{-t_{mn}\pi z}\frac{1-e^{-2t_{mn}}\pi(1-z)}{1-e^{-2t_{mn}\pi}} \leq e^{-t_{mn}\pi z} \ , \tag{48}$$

and

$$a_{mn} = 4\int_0^1\int_0^1 f(x,y)\sin(m\pi x)\sin(n\pi y)dxdy \leq 4M \ . \tag{49}$$

The discrete analog of (45) becomes

$$\begin{array}{rcll} \Delta_h u_h(x,y,z) &=& 0 & \text{in } \Omega_h \\ u_h(x,y,z) &=& 0 & \text{on } \partial\Omega_h \ , \quad z>0 \\ u_h(x,y,0) &=& f_h(x,y) & \text{on } \partial\Omega_h \ , \quad z=0 \end{array} \tag{50}$$

where Δ_h denotes the 7-point stencil (3) and $h = \frac{1}{N}$ the mesh size. The solution of (50) is given by

$$\begin{array}{rcll} u_h^*(x,y,z) &=& \displaystyle\sum_{m=1}^{N-1}\sum_{n=1}^{N-1} b_{mn}(N)\sin(m\pi x)\sin(n\pi y)T(\mu_{mn},z) & \text{for} \quad 0\leq x,y\leq 1, \quad z>0 \\ u_h^*(x,y,z) &=& f(x,y) & \text{for} \quad 0\leq x,y\leq 1, \quad z=0 \end{array} \tag{51}$$

with

$$b_{mn}(N) = \frac{4}{N^2}\sum_{i=1}^{N}\sum_{j=1}^{N} f\left(\frac{i}{N},\frac{j}{N}\right)\sin\left(\frac{m\pi i}{N}\right)\sin\left(\frac{m\pi j}{N}\right) \ . \tag{52}$$

This expansion for the discrete solution is analogous to the continuous Fourier expansion (46). In the following, we will analyze the difference between the two. The parameters t_{mn} of (46) correspond to μ_{mn} of (51). In the next lemmas we will prove the existence of an asymptotic expansion for the real parameters μ_{mn} and the difference of the functions $T(t_{mn}, z) - T(\mu_{mn}, z)$. After that we will continue with the main proof and justify the existence of the representation of u_h^* by (51).

Lemma 1 *The real number μ_{mn} is implicitly defined by*

$$\sinh^2\left(\frac{\mu_{mn}\pi}{2N}\right) = \sin^2\left(\frac{m\pi}{2N}\right) + \sin^2\left(\frac{n\pi}{2N}\right), \quad 0\leq m\leq N-1, \quad 0\leq n\leq N-1 \ . \tag{53}$$

Proof: This follows, since u_h must satisfy the 7-point difference equation at every grid point

$$\begin{aligned}\frac{1}{h^2}(u_h^*(x+h,y,z)+u_h^*(x-h,y,z)+u_h^*(x,y+h,z)+u_h^*(x,y-h,z)\\ +u_h^*(x,y,z+h)+u_h^*(x,y,z-h)-6u_h^*(x,y,z)) &= 0 \ .\end{aligned}$$

Substituting (51), each term of the expansion must satisfy

$$\begin{aligned}&\sin(m\pi(x+h))\sin(n\pi y)\sinh(\mu_{mn}\pi(1-z))+\sin(m\pi(x-h))\sin(n\pi y)\sinh(\mu_{mn}\pi(1-z))\\ +&\sin(m\pi x)\sin(n\pi(y+h))\sinh(\mu_{mn}\pi(1-z))+\sin(m\pi x)\sin(n\pi(y-h))\sinh(\mu_{mn}\pi(1-z))\\ +&\sin(m\pi x)\sin(n\pi y)\sinh(\mu_{mn}\pi(1-z+h))+\sin(m\pi x)\sin(n\pi y)\sinh(\mu_{mn}\pi(1-z-h))\\ -&6\sin(m\pi x)\sin(n\pi y)\sinh(\mu_{mn}\pi(1-z))=0 \ .\end{aligned}$$

This simplifies to

$$\begin{aligned}&\sinh(\mu_m n\pi(1-z))\left(2\sin(m\pi x)\cos(m\pi h)\sin(n\pi y)+\sin(m\pi x)2\sin(n\pi y)\cos(n\pi h)\right)\\ =&\sin(m\pi x)\sin(n\pi y)\left(-2\sinh(\mu_{mn}\pi(1-z))\cosh(\mu_{mn}\pi h)+6\sinh(\mu_{mn}\pi(1-z))\right)\end{aligned}$$

or

$$2\cos(m\pi h)+2\cos(n\pi h)=-2\cosh(\mu_{mn}\pi h)+6 \ , \tag{54}$$

$$\cosh(\mu_{mn}\pi h)-1=1-\cos(m\pi h)+1-\cos(n\pi h) \ . \tag{55}$$

This is equivalent to (53) and proves the lemma.
□

Lemma 2 *μ_{mn} satisfies the estimate*

$$\alpha(m+n)\leq\mu_{mn}\leq m+n \tag{56}$$

with $\alpha=\frac{1}{\pi}\,\mathrm{arsinh}(\sqrt{2})$.

Proof: If we set $p=\frac{\mu_{mn}\pi}{2N}$, $q_1=\frac{\pi m}{2N}$ and $q_2=\frac{\pi n}{2N}$ in (53) we can define p as a function of q_1 and q_2

$$p(q_1,q_2)=\mathrm{arsinh}(\sqrt{\sin^2(q_1)+\sin^2(q_2)}),\quad 0\leq q_1\leq\frac{\pi}{2},\quad 0\leq q_2\leq\frac{\pi}{2} \ . \tag{57}$$

The lemma follows directly by elementary analysis of $p(q_1,q_2)$.
□

Lemma 3 *μ_{mn} has an asymptotic expansion of the form*

$$\mu_{mn}=\sqrt{m^2+n^2}+\sum_{l=1}^{p}c_{lmn}\left(m^2+n^2\right)^{2l}h^{2l}+\mathcal{O}(h^{2p+2}) \ , \tag{58}$$

where c_{lmn} is a bounded polynomial in m,n.

Proof: Since $h=\frac{1}{N}$ we obtain from (57)

$$\mu_{mn}=\frac{2}{\pi h}\mathrm{arsinh}(\Psi_{mn}(h)) \ , \tag{59}$$

where

$$\Psi_{mn}(h)=\sqrt{\sin^2(\frac{\pi mh}{2})+\sin^2(\frac{\pi nh}{2})} \ . \tag{60}$$

By using the series expansions of

$$(\sin(z))^2 \quad = \quad \left(\sum_{i=0}^{\infty}(-1)^i\frac{z^{2i+1}}{(2i+1)!}\right)^2=\sum_{i=0}^{\infty}\frac{(-1)^i2^{2i+1}}{(2i+2)!}z^{2i+2}=\sum_{i=0}^{\infty}\gamma_i z^{2i+2}$$

we get

$$\begin{aligned}
\Psi_{mn}(h) &= \sqrt{\sum_{i=0}^{\infty}\gamma_i\left(\frac{\pi}{2}\right)^{2i+2}\left(m^{2i+2}+n^{2i+2}\right)h^{2i+2}} \\
&= \sqrt{\left(\frac{\pi}{2}\right)^{2}\left(m^{2}+n^{2}\right)h^{2}+\sum_{i=1}^{\infty}\gamma_i\left(\frac{\pi}{2}\right)^{2i+2}(m+n)^{2i+2}h^{2i+2}} \\
&= h\left(\frac{\pi}{2}\right)\sqrt{m^2+n^2}\sqrt{1+\sum_{i=1}^{\infty}\gamma_i\left(\frac{\pi}{2}\right)^{2i}\left(\frac{m^{2i+2}+n^{2i+2}}{m^2+n^2}\right)h^{2i}}\ .
\end{aligned}$$

Now we use

$$(1+z)^{\alpha}=\sum_{k=0}^{\infty}\left(\begin{array}{c}\alpha\\ k\end{array}\right)z^k \tag{61}$$

to get

$$\Psi_{mn}(h) = h\left(\frac{\pi}{2}\right)\sqrt{m^2+n^2}\sum_{k=0}^{\infty}\left(\begin{array}{c}1/2\\ k\end{array}\right)\left(\sum_{i=1}^{\infty}\gamma_i\left(\frac{\pi}{2}\right)^{2i}\left(\frac{m^{2i+2}+n^{2i+2}}{m^2+n^2}\right)h^{2i}\right)^k\ .$$

That is an asymptotic expansion for $\Psi_{mn}(h)$. Furthermore using

$$\operatorname{arsinh}(z)=\sum_{\nu=0}^{\infty}\frac{(-1)^{\nu}(2\nu)!}{2^{2\nu}(\nu!)^2(2\nu+1)}z^{2\nu+1}=\sum_{\nu=0}^{\infty}\lambda_{\nu}z^{2\nu+1} \tag{62}$$

and setting $\beta_k=\left(\begin{array}{c}1/2\\ k\end{array}\right)$ and $\overline{\gamma_i}=\gamma_i\left(\frac{\pi}{2}\right)^{2i}$ we obtain

$$\begin{aligned}
\mu_{mn} &= \frac{2}{\pi h}\sum_{\nu=0}^{\infty}\lambda_{\nu}\left(\Psi_{mn}(h)\right)^{2\nu+1} \\
&= \frac{2}{\pi h}\sum_{\nu=0}^{\infty}\lambda_{\nu}\left(h\left(\frac{\pi}{2}\right)\sqrt{m^2+n^2}\sum_{k=0}^{\infty}\beta_k\left(\sum_{i=1}^{\infty}\overline{\gamma_i}\left(\frac{m^{2i+2}+n^{2i+2}}{m^2+n^2}\right)h^{2i}\right)^k\right)^{2\nu+1} \\
&= \sqrt{m^2+n^2}+\sqrt{m^2+n^2}\sum_{k=1}^{\infty}\beta_k\left(\sum_{i=1}^{\infty}\overline{\gamma_i}\left(\frac{m^{2i+2}+n^{2i+2}}{m^2+n^2}\right)h^{2i}\right)^k \\
&+ \sqrt{m^2+n^2}\sum_{\nu=1}^{\infty}\lambda_{\nu}\left(\sum_{k=0}^{\infty}\beta_k\left(\sum_{i=1}^{\infty}\overline{\gamma_i}\left(\frac{m^{2i+2}+n^{2i+2}}{m^2+n^2}\right)h^{2i}\right)^k\right)^{2\nu+1}\ .
\end{aligned}$$

In the last line one can easily verify that we have only even powers of h in the asymptotic expansion of μ_{mn}. If we factor out $\left(m^2+n^2\right)^{2l}$ for a given h^{2l} then c_{lmn} is bounded for $m,n\to\infty$ since it contains only negative powers of polynomials in m,n. This completes the proof.
□

Lemma 4 *$T(\mu_{mn},z)-T(t_{mn},z)$ has an asymptotic expansion with*

$$T(\mu_{mn},z)-T(t_{mn},z)=T(t_{mn},z)\sum_{l=1}^{p}c_{lmn}\left(m^2+n^2\right)^{2l}h^{2l}+\mathcal{O}(h^{2p+2})\ . \tag{63}$$

Proof: Taylor expansion of $T(\mu_{mn},z)$ gives

$$T(\mu_{mn},z)=T(t_{mn},z)+\sum_{i=1}^{\infty}\frac{1}{i!}\sum_{j=0}^{i}\left(\begin{array}{c}i\\ j\end{array}\right)\left(\frac{\partial^j}{\partial m^j\partial n^{i-j}}T(t_{mn},z)\right)\left(\mu_{mn}-\sqrt{m^2+n^2}\right)^i \tag{64}$$

The partial derivatives of $T(t_{mn}, z)$ are

$$\begin{aligned}
\frac{\partial T(t_{mn}, z)}{\partial m} &= \frac{\sinh(\sqrt{m^2+n^2}\pi)\cosh(\sqrt{m^2+n^2}\pi(1-z))\frac{m}{\sqrt{m^2+n^2}}\pi(1-z)}{\left(\sinh(\sqrt{m^2+n^2}\pi)\right)^2} \\
&- \frac{\cosh(\sqrt{m^2+n^2}\pi)\sinh(\sqrt{m^2+n^2}\pi(1-z))\frac{m}{\sqrt{m^2+n^2}}\pi}{\left(\sinh(\sqrt{m^2+n^2}\pi)\right)^2} \\
&= T(t_{mn}, z)C_m(t_{mn}, z)
\end{aligned}$$

with

$$\begin{aligned}
C_m(t_{mn}, z) &= \coth(\sqrt{m^2+n^2}\pi(1-z))\frac{m}{\sqrt{m^2+n^2}}\pi(1-z) \\
&- \coth(\sqrt{m^2+n^2}\pi)\frac{m}{\sqrt{m^2+n^2}}\pi \\
&\leq \coth(\sqrt{m^2+n^2}\pi(1-z))\pi(1-z) \\
&- \coth(\sqrt{m^2+n^2}\pi)\pi \\
&= C_n(t_{mn}, z)
\end{aligned}$$

and analog $\frac{\partial T(t_{mn}, z)}{\partial n} = T(t_{mn}, z)C_n(t_{mn}, z)$. For $i, j \geq 1$ we thus get

$$\frac{\partial^i}{\partial m^j \partial n^{i-j}} T(t_{mn}, z) = T(t_{mn}, z) R_i \left(C_m, \frac{\partial C_m}{\partial m}, \ldots, \frac{\partial^{i-1} C_m}{\partial m^{i-1}} \right) . \tag{65}$$

We can estimate $C_m(t_{mn}, z)$ by using

$$\coth(kz) = \frac{e^{kz}+e^{-kz}}{e^{kz}-e^{-kz}} = 1 + \frac{2}{e^{2kz}-1} \tag{66}$$

and

$$\frac{d^j}{dz^j}\coth(kz) = r_j \sum_{i=1}^{j+1} \frac{\alpha_i^j}{(e^{2kz}-1)^i} \ , \tag{67}$$

where

$$\begin{aligned}
\alpha_i^j &= i\alpha_i^{j-1} + (i-1)\alpha_{i-1}^{j-1} \ , \quad \alpha_{j+1}^{j-1} = 0 \ , \quad j \geq 2, \ 1 \leq i \leq j+1 \\
r_j &= -2kr_{j-1} \ , \quad j \geq 2 \\
\alpha_1^1 &= \alpha_2^1 = 1, \ r_1 = -4k \ .
\end{aligned}$$

This is shown by induction in [11], p. 24f. Therefore $\frac{\partial^i C_m(t_{mn}, z)}{\partial m^i}$ are bounded for $i \geq 1$. We now insert (58) and (65) into (64)

$$\begin{aligned}
T(\mu_{mn}, z) &= T(t_{mn}, z) \\
&+ T(t_{mn}, z)\sum_{i=1}^{\infty}\frac{1}{i!}\sum_{j=0}^{i}\binom{i}{j} R_i\left(C_m, \frac{\partial C_m}{\partial m}, \ldots, \frac{\partial^{i-1} C_m}{\partial m^{i-1}}\right) \\
&\cdot \left(\sum_{l=1}^{p} c_{lmn}\left(m^2+n^2\right)^{2l} h^{2l} + \mathcal{O}(h^{2p+2})\right)^i
\end{aligned}$$

and simplify the term. This gives (63).
□

Next we consider the discretization error that is the difference between analytical and numerical solution

$$\begin{aligned} u^*(x,y,z) - u_h^*(x,y,z) &= \sum_{m=1}^{\infty}\sum_{n=1}^{\infty} a_{mn}\sin(m\pi x)\sin(n\pi y)T(t_{mn},z) \\ &- \sum_{m=1}^{N-1}\sum_{n=1}^{N-1} b_{mn}(N)\sin(m\pi x)\sin(n\pi y)T(\mu_{mn},z) \\ &= I_1(x,y,z,h) + I_2(x,y,z,h) + I_3(x,y,z,h)\ , \end{aligned}$$

where

$$\begin{aligned} I_1(x,y,z,h) &= \sum_{m=N}^{\infty}\sum_{n=N}^{\infty} a_{mn}\sin(m\pi x)\sin(n\pi y)T(t_{mn},z) && (68)\\ &+ \sum_{m=1}^{N-1}\sum_{n=N}^{\infty} a_{mn}\sin(m\pi x)\sin(n\pi y)T(t_{mn},z) && (69)\\ &+ \sum_{m=N}^{\infty}\sum_{n=1}^{N-1} a_{mn}\sin(m\pi x)\sin(n\pi y)T(t_{mn},z) && (70)\\ I_2(x,y,z,h) &= \sum_{m=1}^{N-1}\sum_{n=1}^{N-1} a_{mn}\sin(m\pi x)\sin(n\pi y)\left\{T(t_{mn},z) - T(\mu_{mn},z)\right\} && (71)\\ I_3(x,y,z,h) &= \sum_{m=1}^{N-1}\sum_{n=1}^{N-1} \{a_{mn} - b_{mn}(N)\}\sin(m\pi x)\sin(n\pi y)T(\mu_{mn},z)\ . && (72) \end{aligned}$$

In the following we try to find an asymptotic expansion in powers of h for these three terms. First we take a closer look at $I_1(x,y,z,h)$ using

$$e^{-x} \le \frac{k!}{x^k} \quad \forall k > 1, \quad x > 0 \tag{73}$$

and $\dfrac{m+n}{2} \le \sqrt{\dfrac{m^2+n^2}{2}} \quad \forall m,n \ge 1$ to get

$$\begin{aligned} |N^s I_1(x,y,z,h)| &\le 4MN^s \sum_{m=N}^{\infty}\sum_{n=N}^{\infty} e^{-\sqrt{2}\sqrt{\frac{m^2+n^2}{2}}\pi z} + 4MN^s \sum_{m=1}^{N-1}\sum_{n=N}^{\infty} e^{-\sqrt{2}\sqrt{\frac{m^2+n^2}{2}}\pi z} \\ &+ 4MN^s \sum_{m=N}^{\infty}\sum_{n=1}^{N-1} e^{-\sqrt{2}\sqrt{\frac{m^2+n^2}{2}}\pi z} \\ &\le 4MN^s \left(\sum_{m=N}^{\infty}\sum_{n=N}^{\infty} e^{-\frac{n\pi z}{\sqrt{2}}} e^{-\frac{m\pi z}{\sqrt{2}}} + \sum_{m=1}^{N-1}\sum_{n=N}^{\infty} e^{-\frac{n\pi z}{\sqrt{2}}} e^{-\frac{m\pi z}{\sqrt{2}}} + \sum_{m=N}^{\infty}\sum_{n=1}^{N-1} e^{-\frac{n\pi z}{\sqrt{2}}} e^{-\frac{m\pi z}{\sqrt{2}}} \right) \\ &= 4MN^s \left(\frac{e^{-\frac{N\pi z}{\sqrt{2}}}}{1-e^{-\frac{\pi z}{\sqrt{2}}}} \frac{e^{-\frac{N\pi z}{\sqrt{2}}}}{1-e^{-\frac{\pi z}{\sqrt{2}}}} + \frac{1-e^{-\frac{N\pi z}{\sqrt{2}}}}{1-e^{-\frac{\pi z}{\sqrt{2}}}} \frac{e^{-\frac{N\pi z}{\sqrt{2}}}}{1-e^{-\frac{\pi z}{\sqrt{2}}}} + \frac{e^{-\frac{N\pi z}{\sqrt{2}}}}{1-e^{-\frac{\pi z}{\sqrt{2}}}} \frac{1-e^{-\frac{N\pi z}{\sqrt{2}}}}{1-e^{-\frac{\pi z}{\sqrt{2}}}} \right) \\ &\le \frac{4Mk!(\sqrt{2})^k}{(\pi z)^k}(1-e^{-\frac{\pi z}{\sqrt{2}}})^{-2}\left(2-e^{-\frac{N\pi z}{\sqrt{2}}}\right)\frac{1}{N^{k-s}} \\ &\le \frac{8Mk!(\sqrt{2})^k}{(\pi z)^k}(1-e^{-\frac{\pi z}{\sqrt{2}}})^{-2}\frac{1}{N^{k-s}}\ . \end{aligned}$$

For every s we can choose a $k > s$ such that

$$\lim_{N\to\infty} |N^s I_1(x,y,z,h)| = 0\ . \tag{74}$$

Therefore $I_1(x,y,z,h)$ has the trivial asymptotic expansion

$$I_1(x,y,z,h) = 0h + 0h^2 + 0h^3 + \ldots \tag{75}$$

Next we derive an asymptotic expansion for $I_2(x,y,z,h)$. We use (58) and (63) to get

$$\begin{aligned} I_2(x,y,z,h) &= \sum_{m=1}^{N-1}\sum_{n=1}^{N-1} a_{mn}\sin(m\pi x)\sin(n\pi y) \\ &\cdot \left(T(t_{mn},z)\sum_{l=1}^{p} c_{lmn}\left(m^2+n^2\right)^{2l}h^{2l}+\mathcal{O}(h^{2p+2})\right) \\ &\leq 4M\sum_{l=1}^{p}\left\{\sum_{m=1}^{N-1}\sum_{n=1}^{N-1} e^{-(m+n)\pi z}c_{lmn}\left(m^2+n^2\right)^{2l}\right\}h^{2l}+\mathcal{O}(h^{2p+2}) \end{aligned}$$

The series $\sum_{m=1}^{\infty}\sum_{n=1}^{\infty} e^{-(m+n)\pi z}c_{lmn}\left(m^2+n^2\right)^{2l}$ converges towards λ_l and therefore we are able to split up the above term

$$\begin{aligned} I_2(x,y,z,h) &\leq 4M\sum_{l=1}^{p}\lambda_l h^{2l}+\mathcal{O}(h^{2p+2}) \\ &+ \left|4M\sum_{l=1}^{p}\sum_{m=N}^{\infty}\sum_{n=1}^{\infty} e^{-(m+n)\pi z}c_{lmn}\left(m^2+n^2\right)^{2l}h^{2l}+\mathcal{O}(h^{2p+2})\right| \\ &+ \left|4M\sum_{l=1}^{p}\sum_{m=1}^{\infty}\sum_{n=N}^{\infty} e^{-(m+n)\pi z}c_{lmn}\left(m^2+n^2\right)^{2l}h^{2l}+\mathcal{O}(h^{2p+2})\right| \\ &= 4M\sum_{l=1}^{p}\lambda_l h^{2l}+\mathcal{O}(h^{2p+2}) \\ &+ \left|4M\sum_{l=1}^{p}\sum_{m=0}^{\infty}\sum_{n=1}^{\infty} e^{-(m+n+N)\pi z}c_{lmn}\left((m+N)^2+n^2\right)^{2l}h^{2l}+\mathcal{O}(h^{2p+2})\right| \\ &+ \left|4M\sum_{l=1}^{p}\sum_{m=1}^{\infty}\sum_{n=0}^{\infty} e^{-(m+n+N)\pi z}c_{lmn}\left(m^2+(n+N)^2\right)^{2l}h^{2l}+\mathcal{O}(h^{2p+2})\right| \\ &\leq 4M\sum_{l=1}^{p}\lambda_l h^{2l}+\mathcal{O}(h^{2p+2}) \\ &+ \left|4M\sum_{l=1}^{p}e^{-N\pi z}N^{2l+2}\sum_{m=0}^{\infty}\sum_{n=1}^{\infty} e^{-(m+n)\pi z}c_{lmn}\left((m+1)^2+n^2\right)^{2l}h^{2l}+\mathcal{O}(h^{2p+2})\right| \\ &+ \left|4M\sum_{l=1}^{p}e^{-N\pi z}N^{2l+2}\sum_{m=1}^{\infty}\sum_{n=0}^{\infty} e^{-(m+n)\pi z}c_{lmn}\left(m^2+(n+1)^2\right)^{2l}h^{2l}+\mathcal{O}(h^{2p+2})\right| \ . \end{aligned}$$

By using (73) and choosing the parameter k high enough we can show that the last two terms are of order $\mathcal{O}(h^{2p+2})$ and therefore $I_2(x,y,z,h)$ has the asymptotic expansion

$$I_2(x,y,z,h)=\sum_{l=1}^{p}\lambda_l h^{2l}+\mathcal{O}(h^{2p+2}) \ . \tag{76}$$

An important fact is that the asymptotic expansion of $I_2(x,y,z,h)$ does not depend on the properties of f.

Finally we look at the third term $I_3(x,y,z,h)$. We have

$$\begin{aligned} I_3(x,y,z,h) &= \sum_{m=1}^{N-1}\sum_{n=1}^{N-1}\{a_{mn}-b_{mn}(N)\}\sin(m\pi x)\sin(n\pi x)T(\mu_{mn},z) \\ &\leq \sum_{m=1}^{N-1}\sum_{n=1}^{N-1}\{a_{mn}-b_{mn}(N)\}\left(T(t_{mn},z)\sum_{l=0}^{p} c_{lmn}\left(m^2+n^2\right)^{2l}h^{2l}+\mathcal{O}(h^{2p+2})\right) \end{aligned}$$

From the **Euler-Maclaurin sum formula** (cf. [20], p. 153 or [21]) we know that in 1D

$$\begin{aligned} a_n - b_n(N) &= 2\left(\int_0^1 f(x)\Psi_n(x)dx - \frac{1}{N}\sum_{i=1}^{N} f(\frac{i}{N})\Psi(\frac{n\pi j}{N})\right) \\ &= -2\sum_{i=1}^{p}\frac{B_{2i}}{(2i)!}h^{2i}\left\{\frac{d^{2i-1}}{dx^{2i-1}}\left[f(x)\Psi_n(x)\right]|_{x=1} - \frac{d^{2i-1}}{dx^{2i-1}}\left[f(x)\Psi_n(x)\right]|_{x=0}\right\} \\ &+ (-1)^p h^{2p+2}\int_0^1 \frac{d^{2p+2}}{dx^{2p+2}}\left[f(x)\Psi_n(x)\right]\sum_{k=1}^{\infty}\frac{2(1-\cos(2\pi kxN)}{(2\pi k)^{2p+2}}dx \ . \end{aligned}$$

It is shown in [11], pp. 34 that this holds for any function f with the above properties and it can be easily extended to higher dimensions. Therefore we can prove in an analog way as for $I_2(x,y,z,h)$ that $I_3(x,y,z,h)$ has an asymptotic expansion of the form

$$I_3(x,y,z,h) = \sum_{l=1}^{p}\theta_l h^{2l} + \mathcal{O}(h^{2p+2}) \ , \tag{77}$$

where θ_l is bounded on Ω. This completes the proof of Theorem 4.

B Proof of Theorem 5

Next we prove Theorem 5 from section 3.2.

Step 1. Assume $f_h = 0$ on Ω. Then we can use the results of appendix A. With (51) and $b_{mn}(N) \le 4M$ we obtain

$$|\partial_x^{2i}\partial_y^{2j}\partial_z^{2k}u_h^*(x,y,z)| \le 4M\pi^{2i+2j}\sum_{m=1}^{N-1}\sum_{n=1}^{N-1} m^{2i}n^{2j}\partial_z^{2k}T(\mu_{mn},z) \ .$$

Using Lemma 3 and the inequalities

$$T(\mu_{mn},z) \le e^{-\mu_{mn}\pi z} \le e^{-\alpha(m+n)\pi z} \tag{78}$$

and

$$\partial_z^{2k}T(\mu_{mn},z) = (\mu_{mn}\pi)^{2k}T(\mu_{mn},z) \le ((m+n)\pi)^{2k}\, e^{-\alpha(m+n)\pi z} \tag{79}$$

we obtain

$$\begin{aligned} |\partial_x^{2i}\partial_y^{2j}\partial_z^{2k}u_h^*(x,y,z)| &\le 4M\pi^{2(i+j+k)}\sum_{m=1}^{N-1}\sum_{n=1}^{N-1} m^{2i}n^{2j}(m+n)^{2k}e^{-\alpha(m+n)\pi z} \\ &\le 4M\pi^{2(i+j+k)}\sum_{m=1}^{\infty}\sum_{n=1}^{\infty} m^{2i}n^{2j}(m+n)^{2k}e^{-\alpha(m+n)\pi z} \end{aligned}$$

This expression is bounded for every i, j, k and does not depend on $h = \frac{1}{N}$. Using the mean value theorem we obtain the same bound for the corresponding finite differences. This proves step 1.

Step 2. Due to the superposition principle it remains to prove the case $g_h = 0$ on $\partial\Omega$. It is easily verified that for the solution of

$$\begin{aligned} \Delta_h v_h &= \delta_x^2 f_h && \text{in } \Omega_h \\ v_h &= f_h && \text{on the left and right edges of } \partial\Omega \\ v_h &= 0 && \text{on the rest of } \partial\Omega \end{aligned}$$

we have the equality

$$v_h = \delta_x^2 f_h \ .$$

This comes from the fact, that the difference equation my be written as

$$\delta_x^2 u_h = f_h - \delta_y^2 u_h - \delta_z^2 u_h \ .$$

and from the uniqueness of the discrete solution. Now we can apply that several times to prove the theorem.

References

[1] Fließbach, T.: Elektrodynamik. 3rd edn. Spektrum Verlag (2000)

[2] Stackgold, I.: Green's Functions and Boundary Value Problems. 2nd edn. John Wiley & Sons (1998)

[3] Walter, W.: Einführung in die Theorie der Distributionen. 3rd edn. BI-Wiss.-Verlag (1994)

[4] Rüde, U.: On the accurate computation of singular solutions of Laplace's and Poisson's equation. Multigrid Methods: Theory, Applications, Supercomputing: Proceedings of the Third Copper Mountain Conference on Multigrid Methods, April 5-10 (1987)

[5] Schwartz, L.: Théorie des Distributions. Hermann, Paris (1978)

[6] Gel'fand, I., Shilov, G.: Generalized Functions. I. Properties and Operations. Academic Press, New York (1964)

[7] Niels, J.: Lineare partielle Differentialgleichungen. Akademie Verlag (1995)

[8] Köstler, H.: Akkurate Behandlung von Singularitäten bei partiellen Differentialgleichungen. Diplomarbeit, Friedrich-Alexander Universität Erlangen-Nürnberg (2003)

[9] Estrada, R., Kanwal, R.P.: Asymptotic Analysis: A Distributional Approach. Birkhäuser, Basel (1994)

[10] Whittaker, E., Watson, G.: A Course of Modern Analysis. 4th edn. Cambridge University Press (1965)

[11] Hofmann, P.: Asymptotic expansions of the discretization error of boundary value problems of the Laplace equation in rectangular domains. Numerische Mathematik **9** (1967) 302–322

[12] Fößmeier, R.: Differenzenverfahren hoher Ordnung für elliptische Randwertprobleme mit gekrümmten Rändern. PhD thesis, Technische Universität München (1984)

[13] Zenger, C., Gietl, H.: Improved schemes for the Dirichtlet problem of Poisson's equation in the neighbourhood of corners. Numerische Mathematik **30** (1978) 315–332

[14] Blum, H., Lin, Q., Rannacher, R.: Asymptotic error expansions and Richardson extrapolation for linear finite elements. Numer. Math. **49** (1986) 11–37

[15] Richardson, L.: The deferred approach to the limit. I. Single lattice. Phil. Trans. Roy. Soc. London A **226** (1927) 229–349

[16] Brandt, A.: On the accurate computation of singular solutions of Laplace's and Poisson's equation. Multigrid Methods: 1984 guide with applications to fluid dynamics, GMD Studie Nr. 85, St. Augustin (1984)

[17] Hackbusch, W.: Multi-Grid Methods and Applications. Springer Verlag (1985)

[18] Trottenberg, U., Oosterlee, C., Schüller, A.: Multigrid. Academic Press (2001)

[19] Rüde, U.: Multiple τ-extrapolation for multigrid methods. Technical Report I-8701, Technische Universität München (1987)

[20] Kronecker, L.: Vorlesungen über Mathematik. (1894)

[21] Olver, F.: Asymptotics and Special Functions. Academic Press, New York (1974)